catalysts

MDPI

Article

Efficient Production of 5-Methoxymethyl-2-furfural from Fructose Catalyzed by Amide-Modified Resin

Chenfeng Li [1,2], Jiahao Ju [3], Beizhan Li [2], Jilei Xu [2,*], Xin Su [2], Zuoyi Xiao [1], Qingda An [1,*] and Jiahui Huang [2,*]

[1] Liaoning Key Lab of Lignocellulose Chemistry and Biomaterials, Liaoning Collaborative Innovation Center for Lignocellulosic Biorefinery, College of Light Industry and Chemical Engineering, Dalian Polytechnic University, Dalian 116034, China; zyxiao80@163.com (Z.X.)
[2] Dalian National Laboratory for Clean Energy, Dalian Institute of Chemical Physics, Chinese Academy of Sciences, Dalian 116023, China; suxin@dicp.ac.cn (X.S.)
[3] Shenhua Engineering Technology Co., Ltd. Anhui Branch, Hefei 23009l, China
* Correspondence: xujilei@dicp.ac.cn (J.X.); anqingda@dlpu.edu.cn (Q.A.); jiahuihuang@dicp.ac.cn (J.H.)

Abstract

5-Methoxymethyl-2-furfural (MMF) serves as a crucial biobased platform molecule that can be transformed into various high-value chemicals and biobased polyester monomers. However, the current production of MMF still faces several challenges, such as low yield and prolonged reaction time. In this study, we prepared a series of amide-modified strongly acidic resin catalysts and discovered that they have a higher efficiency in converting fructose to prepare MMF in 1-Butyl-3-methylimidazolium chloride ([BMIM]Cl) and methanol. Among the synthesized catalysts, DB757-NMP demonstrated superior performance, achieving an MMF yield of approximately 61.5% under the optimized conditions, with a combined yield of HMF and MMF reaching about 66.6%. The catalyst formation mechanism was analyzed using FTIR, and NMR, confirming the transformation of proton between NMP and the sulfonic acid groups of the resin, which collectively promoted the conversion of fructose to MMF. In addition, we investigated main reasons for catalyst deactivation and successfully restored catalytic activity through regeneration. The regenerated catalyst could be reused for three times with only a slight decrease in MMF yield. The results suggested that DB757-NMP is a more sufficient and recyclable catalyst for the production of MMF from fructose. This work presented a simple and environmentally benign approach for the synthesis of MMF.

Keywords: 5-methoxymethyl-2-furfural; dehydration; etherification; fructose; ion-exchange resin

Check for updates

Academic Editor: Ines Graca

Received: 5 February 2026
Revised: 13 March 2026
Accepted: 13 March 2026
Published: 15 March 2026

Copyright: © 2026 by the authors. Licensee MDPI, Basel, Switzerland. This article is an open access article distributed under the terms and conditions of the Creative Commons Attribution (CC BY) license.

1. Introduction

The use of fossil energy has made significant contributions to the development of human society. However, problems such as the greenhouse effect and environmental pollution caused by excessive use of fossil energy cannot be ignored. Using renewable energy to replace fossil energy and reduce environmental problems has become the focus of attention in recent years [1]. Among various renewable resources, biomass resources, due to their large reserves, carbon neutrality, and low cost, are regarded as potential alternatives to fossil energy [2–4]. In biomass resources, 5-Hydroxymethylfurfural (HMF), which could be obtained through the dehydration reaction of carbohydrates, is an important bio-based platform molecule [5,6]. The hydroxyl and aldehyde groups on HMF can undergo various chemical reactions such as oxidation, reduction, and etherification [7–9]. For example, the oxidation product 2,5-furandicarboxylic acid (FDCA) can be widely used as monomer in

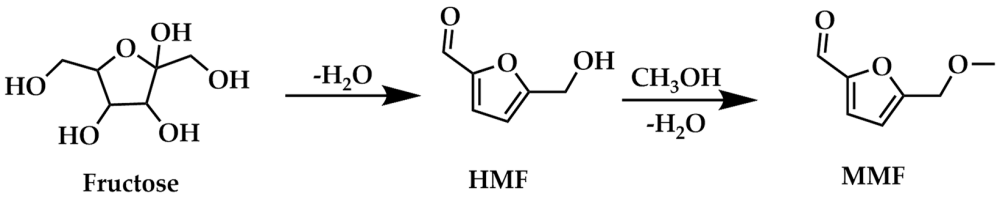
various polymerization fields. FDCA can synthesize Polyethylene furanoate (PEF), which is considered an ideal substitute for Polyethylene terephthalate (PET). However, because of the presence of both hydroxymethyl and aldehyde groups on the furan ring, HMF exhibits highly active chemical properties and can undergo various reactions even at relatively low temperatures. This inherent instability leads to high production and storage costs, thereby limiting the large-scale industrial utilization of HMF [10,11].

5-Methoxymethyl-2-furfural (MMF) is the etherification product of HMF and methanol, with a structure similar to HMF. Compared with HMF, it has more stable chemical stability and lower storage and separate costs. Carro et al. [12]. successfully converted MMF into FDCA through a cascade reaction of oxidoreductases. This indicated that MMF may replace HMF as a new intermediate in furan compound reactions. Up to now, there have been two routes for the preparation of MMF. One is using chloromethyl furfural (CMF) through the William Menzon synthesis method to obtain MMF. However this method will generate hydrochloric acid in the reaction system, which will corrode the equipment and increase the occurrence of side reactions [13]. The other is the HMF etherification reaction to synthesize MMF. This route can achieve a higher MMF yield and has received more research [14]. For instance, P. Diaz Maiz Kurrena et al. achieved a maximum MMF yield of 97% in a batch reactor using ZSM-5 zeolite catalyst [15]. However, due to the high instability of HMF, using HMF to prepare MMF may have a high usage cost, so it is crucial to prepare MMF using inexpensive and widely available biomass raw materials like fructose. Bicker et al. [16]. studied the production of MMF using hydrochloric acid, a liquid acid catalyst, and the MMF yield reached 40% at 120 °C, which suggested that temperature was a key factor for the synthesis of MMF. Kraus and Guney [17] utilized strongly acidic ionic liquids as catalysts for the conversion of fructose to MMF, achieving lower yields. However, by introducing hexane to form a biphasic system consisting of hexane and ionic liquid, the yield of MMF was increased to 57%. Heterogeneous catalysts are more attractive due to their facile separation. Zhang et al. [18]. reported a sulfonated porous polymer catalyst that converted fructose to EMF and MMF in yield of 67.5% and 31.6%, respectively. Both EMF and MMF are etherification products of HMF. However, the preparation of EMF usually requires a longer reaction time, and EMF has a higher boiling point, resulting in higher separation energy consumption compared to MMF. At present, there are still relatively few reports related to MMF, efficient production of MMF from fructose remains an important issue. Therefore, it is of great practical significance to find a method that can produce a considerable yield of MMF.

Ion exchange resin is a kind of high-molecular polymer with a three-dimensional network structure, which is widely used in chemical catalysts and other fields. The acidity of acidic ion exchange resin mainly comes from the sulfonic acid groups grafted on the copolymer skeleton; it plays an important role in the transformation of biomass [19,20]. Zhu and Yang et al. [21,22], conducted a study on the conversion of fructose to MMF using Amberlyst-15 ion exchange resin. They achieved MMF yields of 38.4% and 80.5% respectively. However, the preparation of MMF still requires a relatively long reaction time (10 h). In recent years, researchers have discovered that modifying catalysts can enable them to have higher catalytic activity, significantly increasing the yield of the target product [23,24]. The conversion of fructose to MMF requires H^+ provided by the resin catalyst. Modifying the resin to enhance its ability to provide protons seems to be a good way to increase the efficiency of preparing MMF. Furthermore, the reaction systems for preparing MMF mostly use DMSO as the co-solvent for the reaction; however, DMSO will generate sulfur-containing compounds under high-temperature conditions, thereby polluting the environment [25]. There is a lack of relevant research on the development of environmentally friendly co-solvents in fructose dehydration etherification. The generation

of by-product humins in the catalytic experiment reduced the recyclability of the catalyst. Therefore, exploring the highly efficient and recyclable catalysts and finding green and environmentally friendly reaction systems have important practical significance.

In this work, we prepared a series of amide-modified resin catalysts and used them to the preparation of MMF from fructose in the environmentally friendly co-solvent of 1-Butyl-3-methylimidazolium chloride ([BMIM]Cl) and methanol (Scheme 1). The resin modified with amide has higher catalytic activity compared to the original resin, and can more effectively promote the dehydration etherification reaction of fructose. Among the amide-modified resin catalysts, the DB757-NMP catalyst has relatively better catalytic activity. Under optimal conditions, the yield of MMF could reach 61.5%, and the total yield of HMF and MMF was about 66.6%. The catalyst formation mechanism was analyzed using FTIR and Nuclear Magnetic Resonance (NMR), confirming the transformation of protons between NMP and the sulfonic acid groups of the resin, which collectively promoted the conversion of fructose to MMF. In addition, we studied the possible reasons for catalyst deactivation and proposed a feasible catalyst regeneration method, which allowed the catalyst to be recycled three times with only a slight decrease in MMF yield. This work provided an efficient, environmentally friendly new method for the dehydration etherification reaction of fructose.



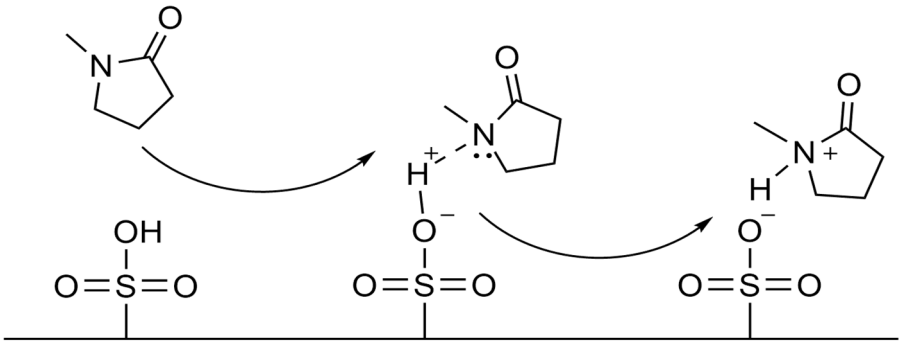
Scheme 1. Reaction pathway for fructose dehydration and etherification.

2. Results and Discussion

2.1. Catalyst Screening

In previous studies, the ionic liquid catalyst obtained from amide and sulfuric acid achieved good results in the conversion of fructose to HMF [26]. However, homogeneous ionic liquids have the disadvantage of being difficult to separate. In this study, we prepared a series of amide-modified resin catalysts and the synthesis mechanism of amide modified resin catalysts was shown in Scheme 2. Then they were used to the preparation of MMF from fructose in the presence of [BMIM]Cl and methanol, and the results were shown in Table 1. It can be observed that in the blank experiment, the dehydration and etherification of fructose remained challenging to achieve without catalytic assistance. (Table 1, entry 1) The conversion rate of fructose and the yield of MMF increased significantly after the introduction of the resin catalyst, which indicated that the dehydration conversion from fructose to MMF needed Brønsted acid. Compared to resin catalysts, when resin catalysts modified with amides (NMP, DMF, and DMA) were used, the yield of MMF was significantly improved (Table 1, entry 2–7, 12, and 13), which indicated that the interactions between amide and sulfonic acid functional groups on the resin could facilitate the selective conversion of fructose to MMF. Compared with other modified catalysts (DB757-DMA, DB757-DMF, DNWII-NMP, and DA330-NMP), DB757-NMP exhibited superior catalytic performance, achieving 100% fructose conversion and MMF yield of 61.5% (Table 1, entry 5–7, 12, and 13). However, when the resin modified with amines was used, the yield of MMF significantly decreased, and HMF became the main product. That was because the basicity of the amine groups neutralized the acidic sulfonic acid sites on the resin, thereby reducing the density of catalytically active protons and diminishing the overall acidity of

the catalyst. Based on the above results, we conducted a detailed study on DB757-NMP in this work.



Scheme 2. Mechanism of synthesis of amide-modified resin catalysts.

Table 1. Dehydration and etherification of fructose catalyzed by resins.

Catalyst	Conversion (%)	MMF Yield (%)	HMF Yield (%)	Total Yield (%)
Blank	34.6	0	0.3	0.3
DB757	100	51.9	15.3	67.2
DNWII	100	55.8	7.8	63.6
DA330	100	54	8.7	62.7
DB757-NMP	100	61.5	5.1	66.6
DB757-DMF	100	60.4	5.2	65.6
DB757-DMA	95.8	61.4	4.4	65.8
DB757-FA	100	16.1	36.4	52.5
DB757-MEA	99.6	6.7	31.8	38.5
DB757-DEA	89.7	0.1	4.9	5.0
DB757-EDA	99.2	19.2	34.6	53.8
DNWII-NMP	100	59.9	3.3	63.2
DA330-NMP	100	60.8	3.5	64.3

Reaction conditions: fructose 100 mg, catalyst 100 mg, MeOH 1.5 g, [BMIM]Cl 0.3 g T = 120 °C, t = 390 min. DMF: N, N-dimethylformamide; DMA: N, N-dimethylacetamide; FA: Formamid; MEA: Monoethanolamine; DEA: Diethanolamine; EDA: Ethylenediamine; NMP: N-Methylpyrrolidone.

2.2. Characterization of the Catalyst

FTIR spectroscopy was used to characterize the ion-exchange resins before and after modification (Figure 1). For the unmodified resin, the characteristic absorption peak observed at approximately 1130 cm^{-1} was attributed to the stretching vibration of the S=O bond, corresponding to the sulfonic acid group of the resin [27]. Additionally, the absorption peaks near 1700 cm^{-1} and 890 cm^{-1} were assigned to the stretching vibrations of the C=C bond in the aromatic ring and the C–O bond, respectively, which were typical features of the resin's carbon skeleton. After modification with NMP, new absorption peaks emerged near 3400 cm^{-1} and 1000 cm^{-1}, which corresponded to the stretching vibrations of the N–H bond and the C–N bond, respectively. This confirmed the successful grafting of NMP onto the resin surface. Furthermore, a noticeable enhancement of the absorption peak at 1700 cm^{-1} was observed after modification. This enhancement could be attributed to the contribution of the C=O stretching vibration from the amide group of the incorporated NMP. Moreover, the S=O stretching vibration peak in the resin from 1130 cm^{-1} was shifting to a lower wavenumber indicated that the electron cloud density of the sulfonic acid group was increased [28,29], which might have proton transfer or hydrogen bond interaction between sulfonic groups and NMP. This interaction was more likely to have facilitated a more efficient conversion of fructose to MMF by optimizing the microenvironment of the catalytic active sites. The XRD patterns of the catalysts were presented in Figure S1.

Both DB757 and DB757-NMP exhibited a broad diffraction feature in the range of 10–37°, which was characteristic of the amorphous carbon of polymeric resins. No peak shifts were observed after modification with NMP. This indicated that the NMP functionalization did not alter the structure of the resin support.

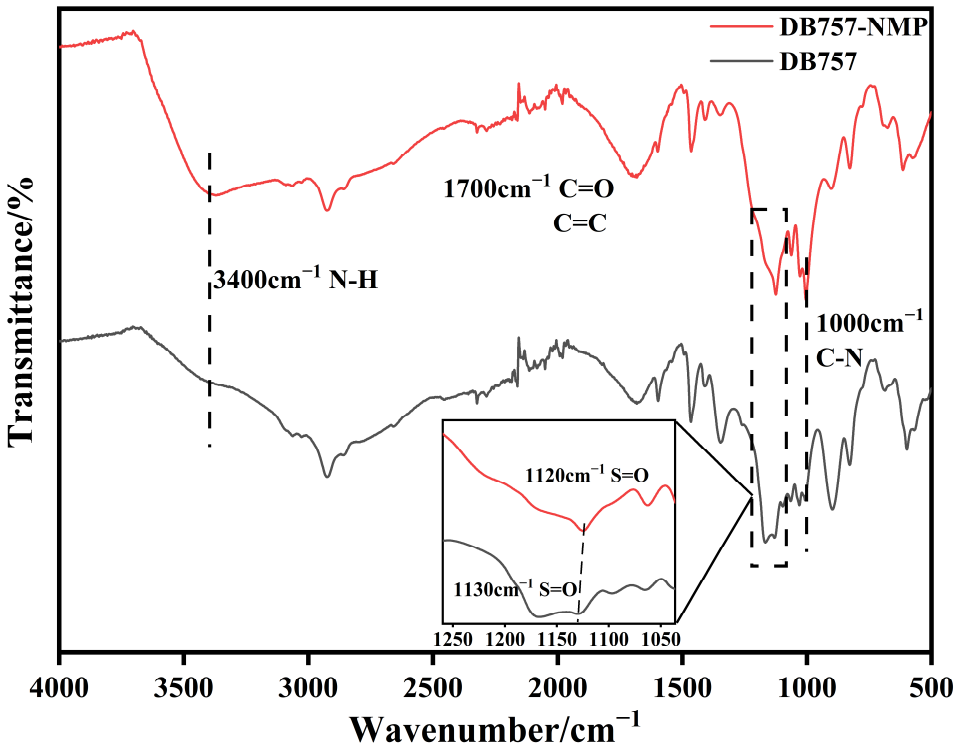


Figure 1. FT-IR Spectra of DB757 and DB757-NMP.

The SEM images (Figure 2) showed that the catalyst has a relative rough surface. The carbon framework in the surface of DB757 resin is composed of many polymer particles, and these particle combinations form the large pore structure on the resin surface. After modification, the structure of the catalyst did not be changed, indicating that the modification has not altered the structural stability of the catalyst. Additionally, the element distribution map showed that the CNOS element was uniformly distributed on the DB757-NMP, proving that NMP has successfully been loaded on DB757 evenly.

Elemental analysis of the modified catalyst is shown in Table 2. After being modified by NMP, the nitrogen content of the catalyst increased to 2.1% compared with DB757, indicating that NMP successfully attached to the surface of the catalyst. Subsequently, the interaction between sulfonic acid groups and NMP was studied through nuclear magnetic resonance (NMR), using p-toluenesulfonic acid (TsOH) and NMP as model substrates; the results were shown in Figure S2. Compared with pure NMP, the chemical shift of hydrogen atoms in NMP mixed with TsOH shifted towards lower fields. This phenomenon indicated that when NMP was mixed with TsOH, the H^+ on the sulfonic acid group transferred to the nitrogen of NMP, forming $[NMPH]^+$, which resulted in a decrease in the electron cloud density around NMP. This phenomenon is consistent with the previous reports of FTIR. These results suggested that when NMP loaded on the DB757, NMP and sulfonic groups on the resin may have formed $[NMPH]^+$ species, which facilitated the production of MMF.

The textural properties of the resin catalysts were investigated using N_2 adsorption–desorption analysis, as shown in Figure 3. Both DB757 and DB757-NMP exhibited type IV adsorption isotherms, accompanied by the formation of H3 hysteresis loops, indicating that the catalysts have macroporous and mesoporous structures. The pore size distribution

was analyzed, and the average pore diameters of DB757 and DB757-NMP were determined to be 60.8 nm and 61.1 nm, respectively. Table 3 showed that both catalysts exhibited lower specific surface areas prior to and following modification. These results indicated that the macroporous properties of the resin were not altered after modification.

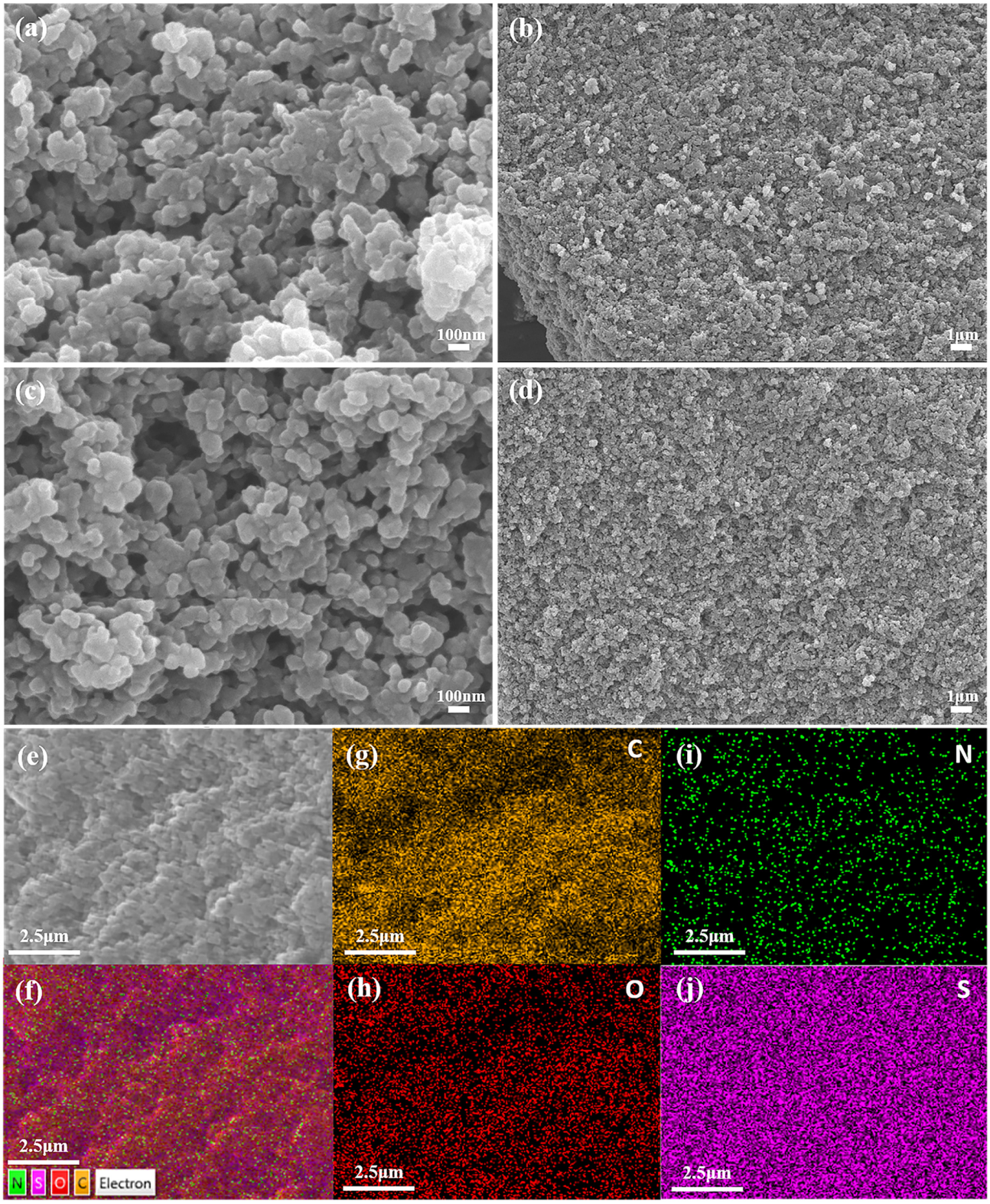


Figure 2. SEM image of DB757 (**a**,**b**) and DB757-NMP (**c**,**d**), EDS image of the DB757-NMP (**e**), C O N S (**f**), C (**g**), O (**h**), N (**i**), S (**j**).

Table 2. Element analysis of the DB757 and DB757-NMP.

Entry	Sample	S%	N%	C%	H%
1	DB757	11.2	0	44.8	5.2
2	DB757-NMP	9.7	2.1	47.8	5.3

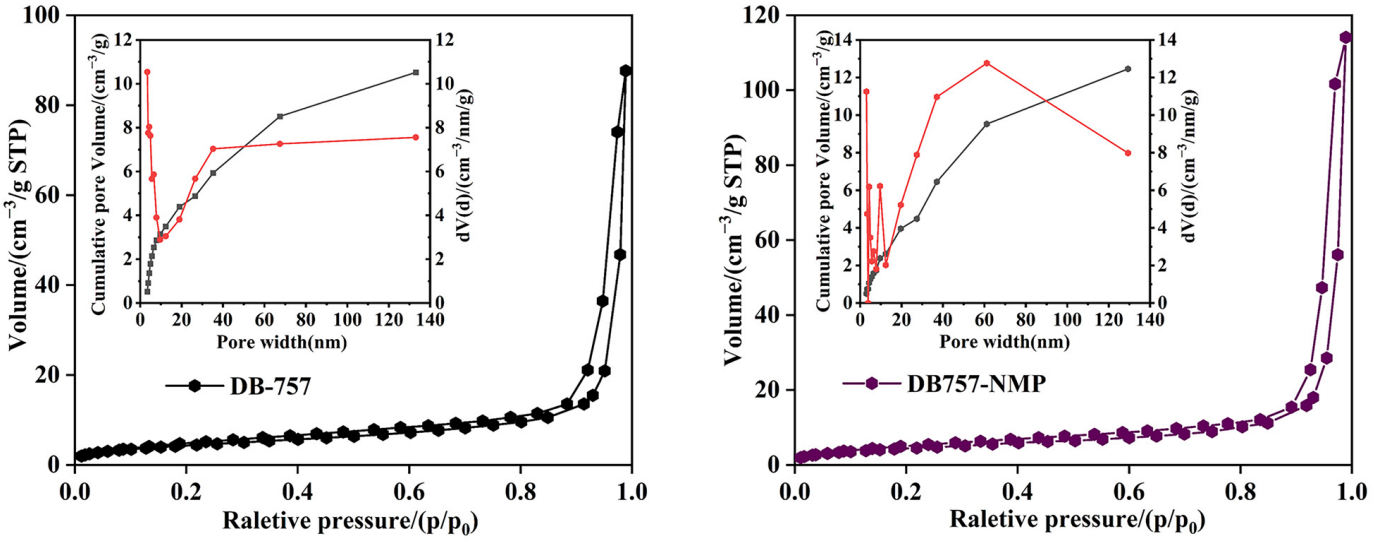


Figure 3. Nitrogen adsorption isotherm of DB757: (**left**) DB757 (black); (**right**) DB757-NMP (purple).

Table 3. Textural characteristics and acid content of catalysts.

Entry	Resin	Surface Area (m^2/g)	Pore Volume (cm^3/g)	Pore Size (nm)	Acid Content (mmol/g)
1	DB757	16.1	0.14	60.8	2.9
2	DB757-NMP	16.7	0.18	61.1	2.55

According to literature reports, the acid capacity of the catalysts were quantified by acid-based titration method [30]. Typically, 0.1 g of the resin catalyst was stirred in 50 mL of a saturated NaCl solution at room temperature, then the catalyst was filtered and rinsed three times with deionized water. All filtrates were combined into a single solution, using phenolphthalein as the indicator, and titrated with a sodium hydroxide solution (2 g/L) while recording the volume consumed. The results were summarized in Table 3. The parent resin DB757 exhibited an acid capacity of 2.9 mmol/g. After modification with NMP, the acid capacity of DB757-NMP decreased to 2.55 mmol/g. This reduction could be attributed to the transformation of a portion of the free hydrogen ions from the sulfonic acid groups into the protonated $[NMPH]^+$ species, as corroborated by the FTIR and NMR analysis.

The TG analysis curves before and after catalyst modification are shown in Figure 4. The weight loss of the two catalysts within 180 °C was mainly due to the decomposition of water on the catalyst surface and the adsorbed water. At temperatures ranging from 250–450 °C, the main reason for the weight loss of DB757 was the decomposition of sulfonic acid groups on the catalyst surface and within the pores. The initial temperature of the second weight loss of the DB757-NMP catalyst was lower than DB757, and the degree of weight loss after 300 °C is higher than DB757, because in the range of 200–450 °C, not only the sulfonic acid groups decomposed, but also the NMP groups loaded on the catalyst. The weight loss of the two catalysts after 450 °C belonged to the decomposition of the numerical carbon skeleton. The TG analysis indicated that this resin catalyst has excellent thermal stability within the operating temperature range.

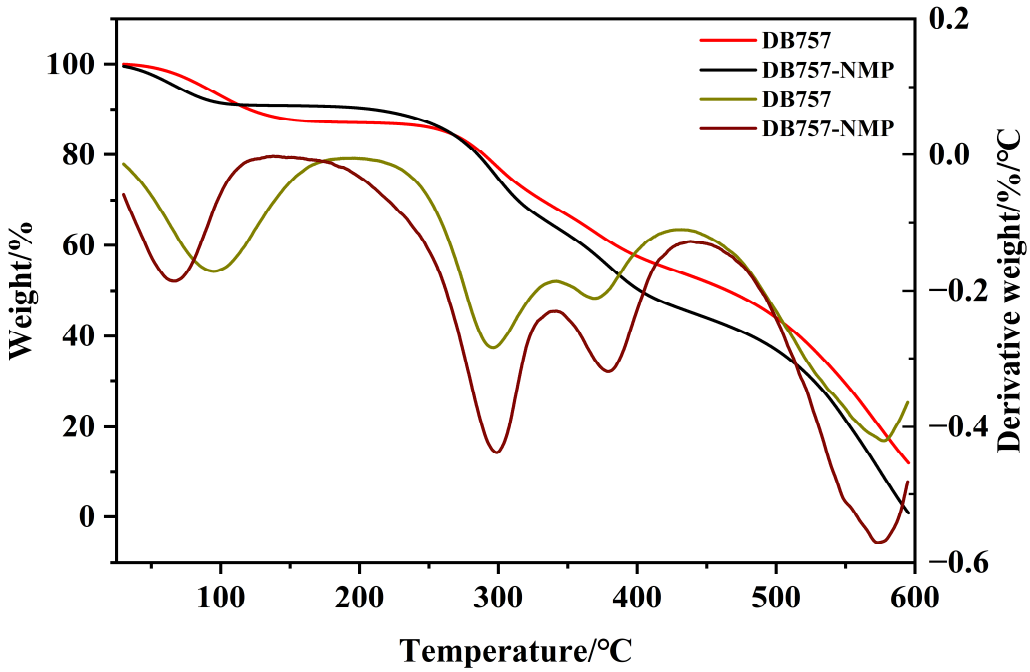


Figure 4. TG analysis of DB757 and DB757-NMP.

2.3. Catalytic Activity of DB757-NMP

The catalytic performance of DB757-NMP in one pot conversion of fructose to MMF in methanol was systematically evaluated, and the effects of key parameters such as reaction temperature, reaction time, catalyst loading, fructose concentration, and different co-solvents on MMF yield were explored in detail.

From Table 4, it was evident that fructose was completely converted when methanol was used as the sole solvent, but the yield of MMF reached only 1.5%. The addition of co-solvents can significantly alter the reaction pathway and microenvironment for the dehydration–etherification process. The influence of various co-solvents on the conversion of fructose to MMF was investigated. When conventional organic solvents were used such as DMSO, NMP, and acetonitrile as co-solvents, moderate yields of MMF could be achieved (Table 4, entry 3–5). To our delight, when an environmentally benign ionic liquid, [BMIM]Cl, was used as a co-solvent to replace the conventional organic solvents, the yield of MMF reached 61.5%, and the combined yield of HMF and MMF reached 66.6%. It was suggested that the strong interactions between ionic liquids and HMF could effectively stabilize the reactive intermediate and facilitated its selective transformation to MMF [31]. In contrast, THF and MIBK were ineffective co-solvents, with almost no MMF detected (Table 4, entry 6 and 7). Therefore, we investigated various factors, including reaction temperature, reaction time, catalyst loading, and fructose concentration, that may affect the yield of MMF using [BMIM]Cl as co-solvent.

As shown in Figure 5a, at a lower reaction temperature, a large portion of fructose has already been converted, and the fructose could be converted completely across the range of 90–130 °C. At 70 °C, the MMF yield was 34%, indicating that DB757-NMP was already active for MMF formation at relatively low temperatures. The yield increased progressively with temperature, reaching 61.5% at 120 °C. However, when the temperature reached 130 °C, the yield of MMF decreased slightly. This decrease was likely due to the instability of intermediate HMF under harsh conditions, where there were side reactions such as polymerization and generating other by-products [32]. Therefore, 120 °C was identified as the optimal reaction temperature for MMF production from fructose.

Table 4. Preparation of MMF from other co-solvent.

Entry	Co-Solvent	Conversion (%)	HMF Yield (%)	MMF Yield (%)
1	None	100	0.2	1.5
2	[BMIM]Cl	100	5.1	61.5
3	DMSO	100	2.4	25.8
4	NMP	100	1.8	41.4
5	MeCN	99.2	2.2	46.5
6	THF	96.6	9.2	0.4
7	MIBK	99.0	1.5	0.4

Reaction conditions: fructose 100 mg, DB757-NMP 100 mg, co-solvent 0.3 g, methanol 1.5 g, 390 min, 120 °C.

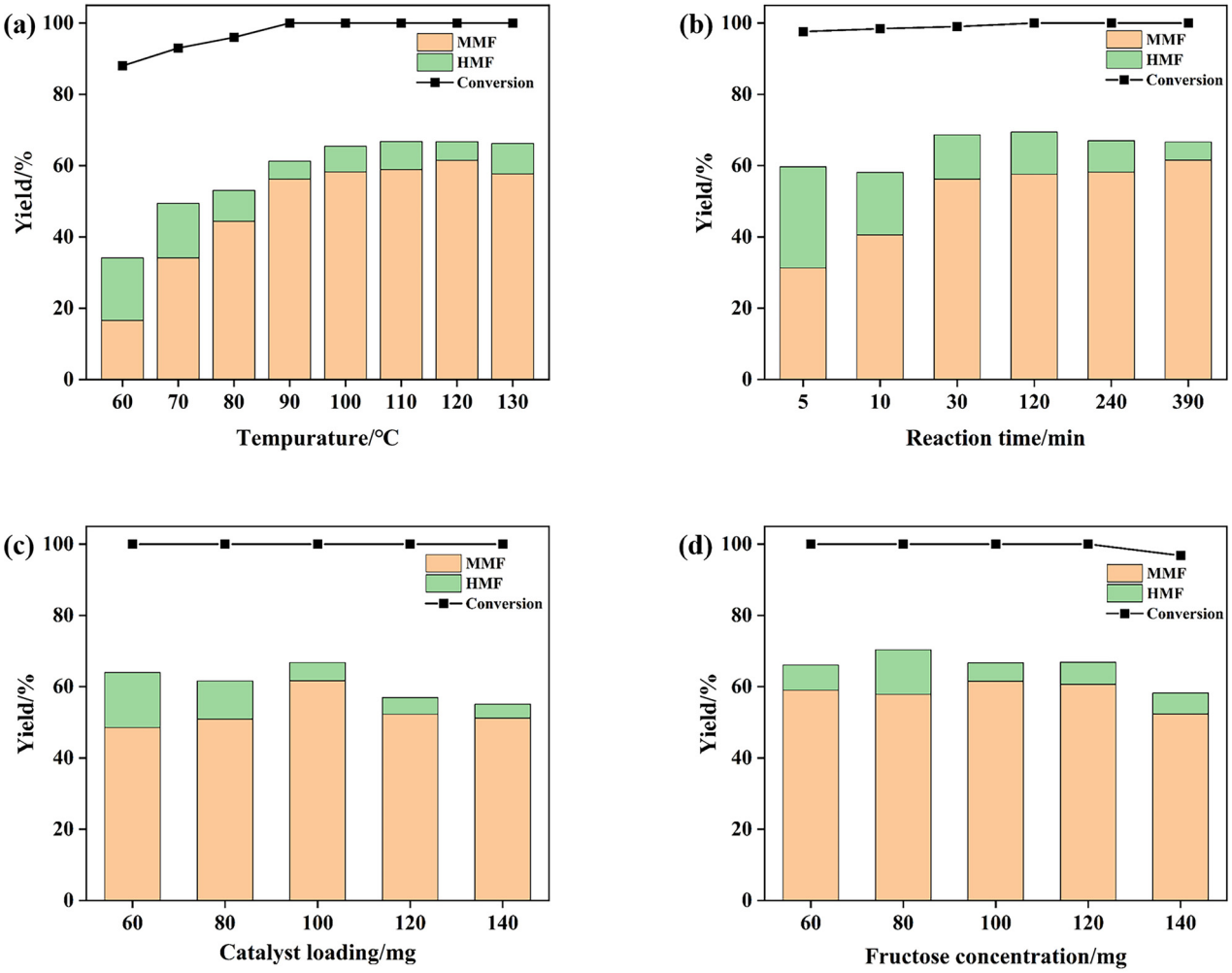


Figure 5. Effects of reaction parameters: (**a**) reaction temperature; (**b**) reaction time; (**c**) catalyst loading; (**d**) fructose concentration on the dehydration and etherification of fructose. Reaction conditions: (**a**) fructose 100 mg, DB757-NMP 100 mg, [BMIM]Cl 0.3 g, methanol 1.5 g, 390 min; (**b**) fructose 100 mg, DB757-NMP 100 mg, [BMIM]Cl 0.3 g, methanol 1.5 g, 120 °C; (**c**) fructose 100 mg, [BMIM]Cl 0.3 g, methanol 1.5 g, 390 min, 120 °C; (**d**) DB757-NMP 100 mg, [BMIM]Cl 0.3 g, methanol 1.5 g, 390 min, 120 °C.

The influence of reaction time on the yield of MMF is illustrated in Figure 5b. Within 30 min, the fructose was almost completely consumed, and the HMF yield displayed a characteristic trend: it initially increased and then gradually decreased. The yield of MMF reached 56.17% at 30 min. This indicated that the dehydration of fructose to HMF was the main and rapid step in the reaction network, and HMF was the main intermediate product. In addition, the yield of MMF had already reached 56% at 30 min, proving that DB757-

NMP has strong dehydration and etherification activity. During the long-term dehydration and etherification reaction, the yield of MMF could increase slowly and still maintained a relatively high level, indicating that MMF possessed considerable stability under the [BMIM]Cl co-solvent system and was not easily consumed by secondary degradation pathways. After 30 min, the MMF yield rose slowly and reached the maximum value of 61.5% at 390 min.

The relationship between catalyst loading and MMF yield was presented in Figure 5. When the catalyst amount was low, the yield of MMF was below 50%, and a relatively high concentration of the intermediate HMF was observed. As the catalyst loading increased, the MMF yield rose progressively, reaching a maximum at a loading of 100 mg. This suggested that the increased density of acid sites adequately promoted both consecutive steps in the reaction cascade. However, a further increase in catalyst loading beyond 100 mg led to a decline in MMF yield. Excessive acidic sites would accelerate adverse reactions, such as the rehydration of HMF or the degradation of MMF [33].

The substrate concentration has a significant impact on the production cost of the product. As shown in Figure 5d, initially, increasing the fructose concentration led to a higher yield of MMF. However, when the fructose concentration was raised from 5wt% to 7wt%, the fructose conversion decreased slightly, MMF yield dropped from 61.5% to 52.3%, and the higher fructose concentration promoted the occurrence of side reactions, thereby forming by-products such as humins. These side reactions competed with the main reaction, consuming fructose and the intermediate HMF, which led to a decrease in the yield of MMF. Consequently, a fructose concentration of 5wt% was identified as the optimal condition of this reaction, and a maximum MMF yield of 61.5% can be achieved.

2.4. Recyclability of DB757-NMP

The recyclability of catalysts is a key performance indicator as it directly determines the actual cost-effectiveness. Although the amide-modified resin demonstrated competence in converting concentrated fructose to MMF, its recyclability was found to be unsatisfactory. As shown in Figure 6, significant deactivation was observed upon the first reuse cycle: the MMF yield drastically dropped from 61.5% to 9% and the product distribution shifted notably, with HMF becoming the major product at a yield of 52.6%. The pronounced formation of HMF suggested a decline in the number and accessibility of acid sites. The possible reason was that during the reaction process, the byproduct humins covered the surface of the catalyst, which physically blocked the active sites and hindered further catalytic cycling, while leaching of -SO_3H occurred on the resin catalyst.

To verify our hypothesis and elucidate the deactivation mechanism, FT-IR analysis was performed on the used catalysts. As shown in Figure 7, the spectrum of the used catalyst revealed a significant decrease in the intensity of the characteristic S=O stretching peak at approximately 1100 cm^{-1}, indicating that sulfonic acid groups might leach out of the resin or be covered by humins. Concurrently, a pronounced enhancement of the C–H stretching vibrations around 2900 cm^{-1} was observed, suggested the deposition of carbonaceous species on the catalyst surface. Furthermore, the appearance of new absorption bands at 3100 cm^{-1}, 1571 cm^{-1}, and 1000 cm^{-1}, attributable to the C–H, C=N, and C–N stretching vibrations of an imidazolium ring, provided evidence for an ion-exchange process during the reaction [34]. This implied that the originally grafted amide-based cations were partially replaced by cations from the ionic liquids in the reaction system. This change was confirmed by the measured acid capacity, which sharply decreased from 2.55 mmol/g of fresh catalyst to 1.1 mmol/g after use (Table 5). In other words, ion exchange during the reaction process might be the main factor causing catalyst deactivation. The XRD pattern (Figure S1) of the used catalyst shifted to a higher diffraction angle compared to that of the fresh catalyst.

This shift could be attributed to the deposition and accumulation of imidazolium cations on the catalyst surface and within its pores.

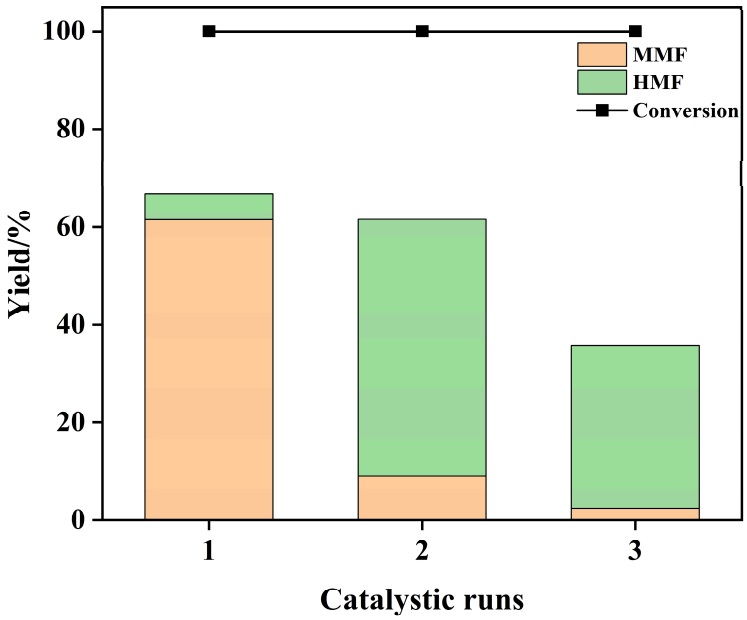


Figure 6. DB757 recycling tests for dehydration and etherification of fructose. Reaction conditions: substrate 100 mg, DB757-NMP 100 mg, [BMIM]Cl 0.3 g, methanol 1.5 g, 390 min, 120 °C.

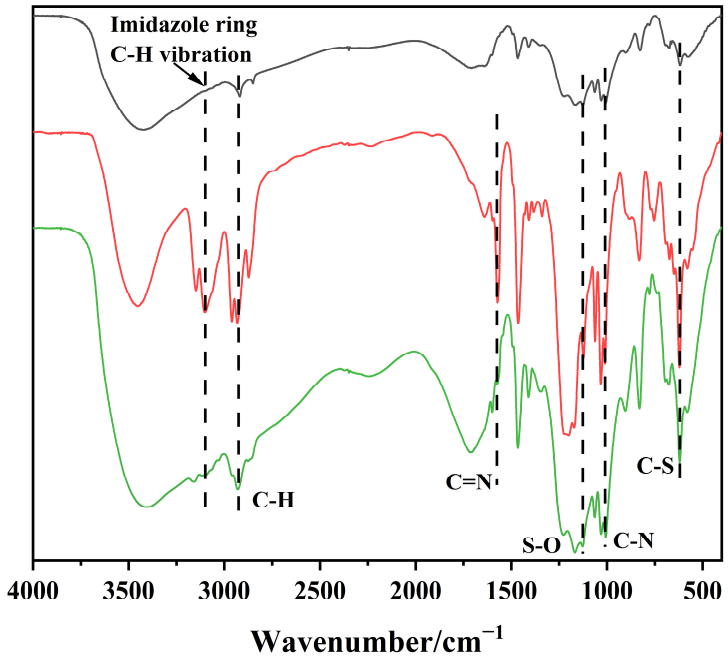


Figure 7. ATR-IR spectra of DB757-NMP (black); used DB757-NMP (red); generated DB757-NMP (green).

Table 5. Textural characteristics and acid content of used/generated catalysts.

Entry	Sample	Surface Area (m^2/g)	Pore Volume (cm^3/g)	Pore Size (nm)	Acid Content (mmol/g)
1	DB757-NMP	16.7	0.18	61.1	2.55
2	Uesd DB757-NMP	16.1	0.20	49.3	1.1
3	Generated DB757-NMP	16.9	0.18	43.8	2.45

The spectroscopic and titration data consistently point to active site loss via sulfonic group leaching, pore blockage by humins, and cation exchange as the primary factors responsible for the irreversible deactivation. Elemental analysis of the used catalyst provided further insight into its deactivation. A significant increase in nitrogen content was observed, rising from 2.1% to 6.2%. This phenomenon supported the occurrence of an ion-exchange process, as interred from FT-IR. Furthermore, the sulfur content decreased from 9.7% to 8.4%, and the carbon content increased from 47.8% to 54.2%, indicating either the leaching of sulfonic acid groups or their coverage by deposited species. Nitrogen physisorption measurements of the used catalyst complemented these findings (Figure 8). The average pore diameter decreased from 61.1 nm to 49.3 nm. This reduction in pore size was likely attributable to the partial blockage of pores by insoluble humins species formed during the reaction and imidazole from [BMIM]Cl, which was consistent with the observation of carbon deposition from other characterizations.

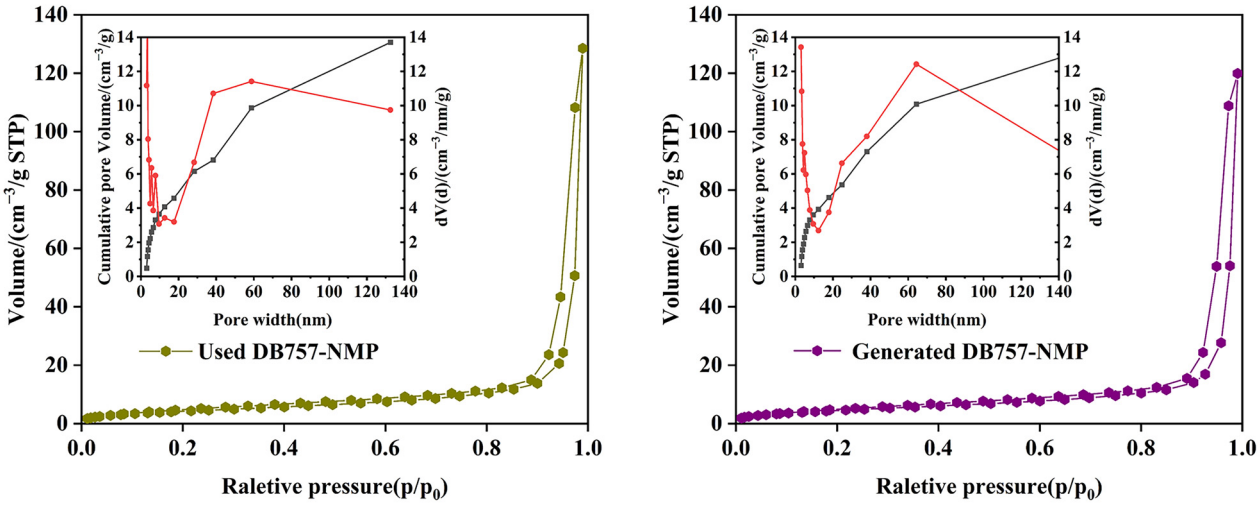


Figure 8. Nitrogen adsorption–desorption isotherm of DB757. (**left**) Used DB757-NMP (green), (**right**) generated DB757-NMP (purple).

To optimize the recyclability of the catalyst, we carried out a regeneration treatment for the deactivated catalyst. Firstly, humins attached to the catalysts need to be removed. We used different elution agents to clean the used DB757-NMP catalyst, and the used catalyst was stirred at room temperature for 24 h to achieve the cleaning purpose. As shown in Table S2, the catalyst after washing still shows low reactivity for the synthesis of MMF. This indicated that it was very difficult for these deactivating agents to remove the humins attached to the catalyst. Therefore, we used the strong oxidant hydrogen peroxide to remove humins attached to the catalyst surface, and used sulfuric acid to regenerate the acidic sites of the catalyst. The catalyst regeneration process was shown in Section 3.3.

The regenerated catalyst was comprehensively characterized to evaluate the effectiveness of the recovery process. Firstly, the XRD pattern (Figure S1) of the regenerated catalyst confirmed that the regeneration procedure successfully restored the structure of the resin support in its initial condition. As shown in the FT-IR spectra (Figure 7), the characteristic peaks associated with the imidazolium cation at approximately 3100 cm^{-1}, 2900 cm^{-1}, and 1571 cm^{-1} disappeared after regeneration. The overall spectral profile closely resembled that of the fresh catalyst, indicating the basic removal of the ionic liquid residues. Elemental analysis revealed that the nitrogen content in the regenerated catalyst decreased from 6.2% in the used catalyst to 3.5% (Table 6). Meanwhile, the sulfur content increased slightly after regeneration, possibly due to a small amount of sulfuric acid remaining in the resin pores.

The above data indicated that through regeneration, the composition and structure of the catalyst had been basically restored to the level of the fresh catalyst.

Table 6. Element analysis of catalysts.

Entry	Sample	S%	N%	C%	H%
1	DB757-NMP	9.7	2.1	47.8	5.3
2	Used/DB757-NMP	8.4	6.2	54.2	6.0
3	Generated DB757-NMP	10.8	3.5	50.2	3.9

The cycling performance of the regenerated catalyst was evaluated, and the results were presented in Figure 9. Compared to the catalyst without regeneration, the regenerated catalyst exhibited improvement in stability, with less decline in MMF yield over the initial three runs. However, the MMF yield dropped in the fourth run. Concurrently, an increasing trend in HMF yield was observed across the four cycles. This observation suggested that the catalyst still suffered from irreversible loss of acid sites even after regeneration, such as the acidic sites covered by humins. The reduction of acidic sites prevented HMF from undergoing effective etherification reactions, thereby lowing the yield of MMF. In summary, the catalyst improved its recyclability after regeneration, demonstrating the effectiveness of catalyst regeneration.

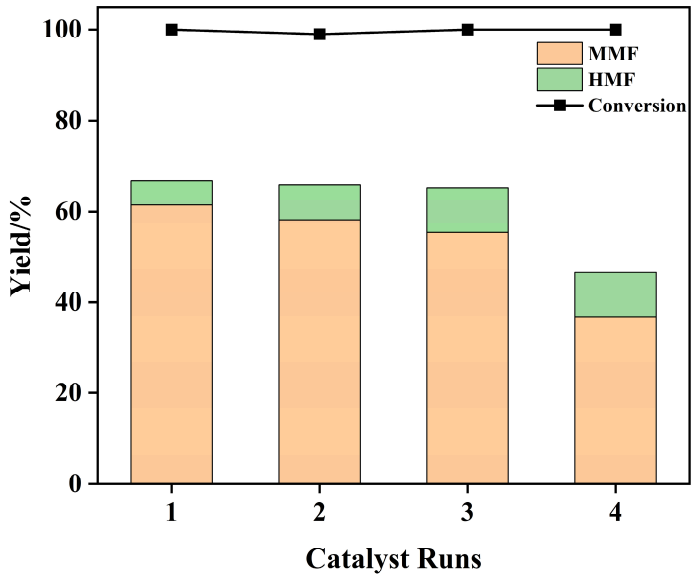


Figure 9. Recycling of regenerated catalyst. Reaction conditions: substrate 100 mg, DB757-NMP 100 mg, [BMIM]Cl 0.3 g, methanol 1.5 g, 390 min, 120 °C.

Subsequently, MMF was fabricated on various substrates under identical conditions, and the results were shown in Figure 10. When glucose was employed as the substrate, only trace amounts of MMF and HMF were detected, because the glucose should first isomerize to fructose then dehydrate to HMF [35]. This isomerization step typically required Lewis acid or base catalysis [36,37]. The trace product formation suggested that the amide groups in the catalyst might offer limited promotion for glucose isomerization. In contrast, when substrates containing fructose units were used, such as sucrose and inulin, the MMF yield increased significantly to 24.2% and 54.6%, respectively. The higher yield from inulin, because it contained a higher proportion of fructose units, which could be converted to HMF directly. These results demonstrated that the present catalytic system exhibited promising activity for the conversion of fructose-containing carbohydrates into MMF.

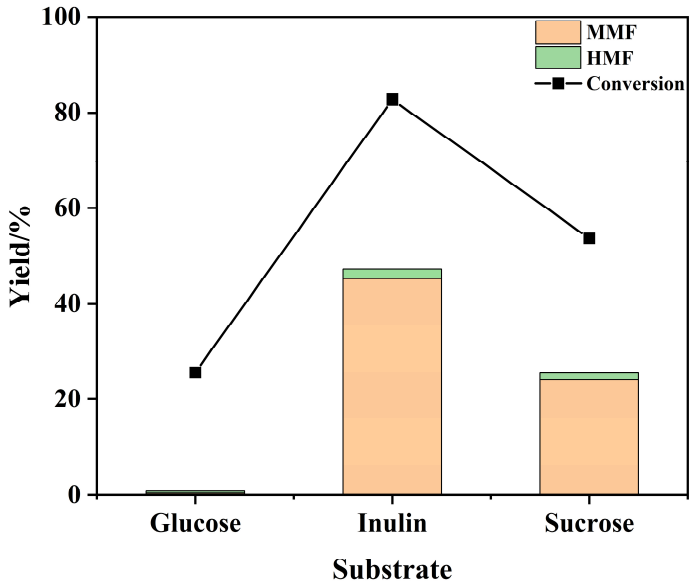
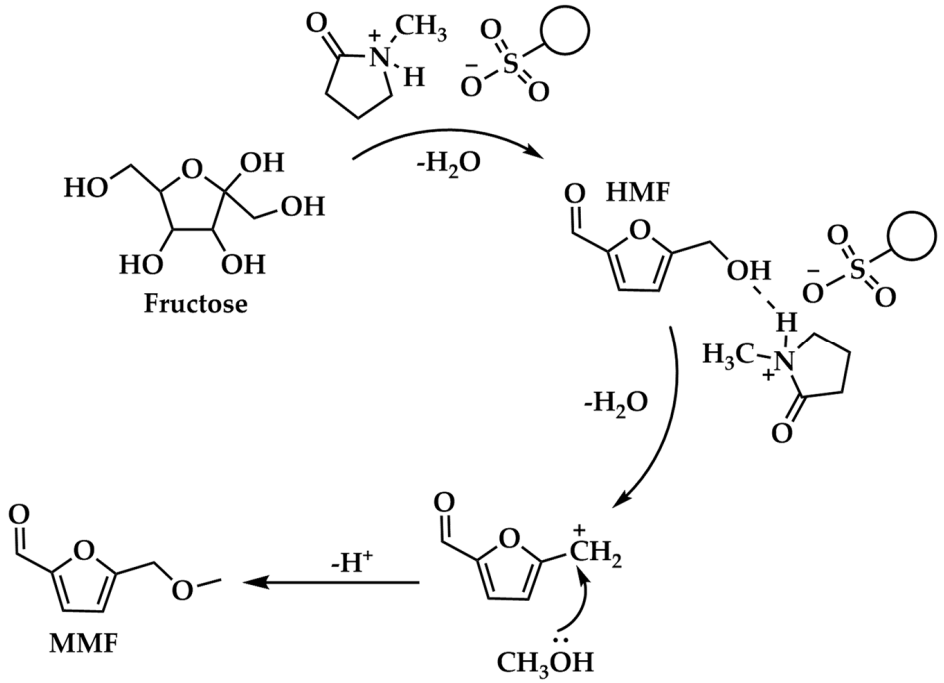


Figure 10. Preparation of MMF from other carbohydrates. Reaction conditions: substrate 100 mg, DB757-NMP 100 mg, [BMIM]Cl 0.3 g, methanol 1.5 g, 390 min, 120 °C.

Based on previous reports and our experimental results, we proposed a possible mechanism for the conversion of fructose to prepare MMF shown in Scheme 3. Firstly, $[NMPH]^+$ species were formed through proton transfer between sulfonic acid groups on the resin and NMP, which could effectively activate and transfer protons in the reaction system [38]. Activated protons could promote the dehydration of fructose to form HMF rapidly. Subsequently, the hydroxyl group of HMF was activated by hydrogen bonding between the lone pair electrons on the HMF hydroxyl group and the H of $[NMPH]^+$. Activated HMF formed an intermediate carbocation after removing a fraction of water. Finally, a nucleophilic addition reaction occurred between the intermediate carbocation iand methanol, resulting in the final product MMF.



Scheme 3. Possible pathway for the preparation of MMF from the dehydration–etherification of fructose catalyzed by DB757-NMP.

3. Materials and Methods

3.1. Materials

Fructose (≥99%), 5-Methoxymethyl-2-furfural (97%), ethanolamine (≥99.0%), Diethanolamine (≥99.0%), and ethylenediamine (≥99.0%) were purchased from Shanghai Aladdin Biochemical Technology Co., Ltd. (Shanghai, China). N,N-Dimethylformamide (≥99%), N,N-Dimethylacetamide (≥99%), and formamid (≥99%) were obtained from Tianjin Kemiou chemical reagent Co., Ltd. (Tianjin, China). Glucose (AR), sucrose (AR), inulin (AR), DMSO (≥99%), tetrahydrofuran (≥99%), and acetonitrile (≥99%) were provided by Sigma-Aldrich Shanghai Trading Co., Ltd. (Shanghai, China). DB757, DNWII, and DA330 were purchased from Dandong Mingzhu Special Type Resin Co., Ltd. (Dandong, China). N-Methylpyrrolidone (99.9%) and 1-Butyl-3-methylimidazolium chloride (99%) were purchased from Beijing InnoChem Science and Technology Co., Ltd. (Beijing, China). THF (≥99%) and Isopropanol (≥99%) were purchased from Tianjin Damao Chemical reagent partnership enterprise (Tianjin, China).

3.2. Preparation of the Catalysts

Amide modified resin catalysts are prepared by the impregnation method. Firstly, the resin was ground into power and sieved through a 100 mesh sieve. Then, 5 g of the resin powder was dispersed into 50 g of deionized water under stirring. Subsequently, an amide aqueous solution containing 5 g of amide was added dropwise to the dispersion mentioned above. The mixture was stirred at room temperature for 24 h. After stirring, the mixture was filtered and washed several times with deionized water until the filtrate was neutral. The washed catalyst was dried overnight at 110 °C to obtain the modified resin catalyst.

3.3. Catalysts Regeneration

The regeneration of the catalyst was as follows: the used catalyst was stirred in a hydrogen peroxide solution at room temperature for 24 h to remove the humins covering the surface of resin, and the solid was then filtered off and thoroughly washed with deionized water. Subsequently, the washed catalyst was subjected to an ion-exchange process by stirring in a dilute sulfuric acid solution for another 24 h. After ion exchange, the solid was washed with deionized water until the pH of the filtrate reached neutral, then the catalyst was dried in an oven at 110 °C overnight. The regenerated support was then functionalized again with NMP following the same procedure used for the initial preparation. The resulting material was denoted as Generated DB757-NMP.

3.4. Catalyst Characterization

X-ray diffraction (XRD) data were collected using an empyrean diffractometer. (Malvern Panalytical, Almelo, The Netherlands) The ATR-IR spectra of the resin were detected in the ATR mode on the Nicolet iS50 infrared spectrometer. (Thermo Fisher Scientific, Waltham, MA, USA) Brunauer–Emmett–Teller (BET) surface areas of the catalyst were obtained from nitrogen physisorption tests. Nitrogen adsorption and desorption isotherms were recorded on an Autosorb1-C/TCD instrument at 77K. (Quantachrome, Boynton Beach, FL, USA) Elemental analysis to assess the carbon, sulfur, nitrogen, and hydrogen was recorded on a Vario EL cube. (Elementar, Frankfurt, Germany) ^{1}H-NMR data were collected using a Bruker advance III 400MHz NMR spectrometer. (Bruker, Karlsruhe, Germany) Thermogravimetry (TG) was carried out on a TA DSC Q2000 instrument (TA Instruments, New Castle, DE, USA) in the range of 30–600 °C and heating rate of 10 °C/min under a N_2 atmosphere. SEM images of DB757 and DB757-NMP were captured using a JSM-6460LV scanning electron microscope. (JEOL Ltd., Tokyo, Japan) EDS images were obtained by a X-Max50 spectrometer. (Oxford Instruments, Oxford, UK)

3.5. Catalytic Performance Test

All carbohydrate catalytic experiments were conducted in 35 mL thick-walled pressure tubes. In a typical reaction, 0.1 g of fructose, 1.5 g of methanol, 0.3 g of ionic liquids, and 0.1 g of catalyst were loaded in the thick-walled pressure tube. The sealed thick-walled pressure tube was placed in an oil bath at the optimal temperature. After the reaction was complete, the reaction tube was placed in an ice water mixture to terminate the reaction. After cooling, the reaction mixture was diluted to 50 mL with deionized water. The product was qualitatively and quantitatively analyzed by high performance liquid chromatography (HPLC) equipped with a Shodex KS-801 (Sugar) HPLC column and the differential refractive index detector (RID) and a variable wavelength detector (VWD) detector using ultrapure water as the mobile phase with a flow rate of 1 mL min^{-1} at 50 °C. The conversion of fructose and the yield of products were calculated according to the following formula:

$$\text{Fructose conversion } (\%) = \frac{(\text{molars of initial fructose} - \text{molars of remained fructose})}{(\text{molars of initial fructose})} \times 100\%$$

$$\text{MMF yield } (\%) = \frac{(\text{molars of produced MMF})}{(\text{molars of initial fructose})} \times 100\%$$

$$\text{HMF yield } (\%) = \frac{(\text{molars of produced HMF})}{(\text{molars of initial fructose})} \times 100\%$$

4. Conclusions

In summary, an amide-modified resin catalyst could facilitate the one-pot preparation of MMF from fructose. When DB757-NMP was used, a 61.5% MMF yield could be obtained under optimal conditions, and the total yield of HMF and MMF can reach 66.6%. Elemental analysis, SEM, and FITR confirmed the successful loading of NMP on the DB757. The diversion of proton between sulfonic acid groups and NMP was characterized using FTIR and ^{1}H-NMR. This proton transfer could promote the conversion of fructose to MMF. The reasons for the catalyst's deactivation had been investigated, and the deposition of humins on the catalyst and the ion exchange of the imidazole groups in the ionic liquid were the main reasons for the deactivation of the catalyst. A regeneration procedure was carried out on the used catalyst, significantly enhancing the catalytic activity of the used catalyst. The catalyst could be recycled three times with only a slight decrease in MMF yield, and the substrate expansion experiment confirmed that the catalytic system could efficiently convert carbohydrates containing fructose components into MMF. Overall, this work presented a simple and environmentally benign method for the preparation of MMF, with potential application prospects in biomass application.

Supplementary Materials: The following supporting information can be downloaded at: https://www.mdpi.com/article/10.3390/catal16030264/s1, Table S1: The abbreviations and their full forms that appear in the article; Figure S1: XRD pattern of catalysts; Figure S2: ^{1}H-NMR of the NMP, [NMPH][TsO]; Table S2: The yield of MMF obtained by washing Used-DB757 with different elution agents.

Author Contributions: Writing—original draft, Investigation, Formal analysis, C.L.; Methodology, Data curation, J.J.; Methodology, B.L.; Writing—review and editing, Supervision, Validation, J.X.; Funding acquisition, X.S.; Review and editing, Supervision, Z.X.; Supervision, Q.A.; Supervision, Funding acquisition, J.H. All authors have read and agreed to the published version of the manuscript.

Funding: This research was funded by National Natural Science Foundation of China—Youth Science Fund (22308347).

Data Availability Statement: The data that support the findings of this study are available from the corresponding author upon reasonable request.

Acknowledgments: The authors have reviewed and edited the output and take full responsibility for the content of this publication.

Conflicts of Interest: Author Jiahao Ju was employed by the company Shenhua Engineering Technology Co., Ltd. An hui branch, Hefei. The remaining authors declare that the research was conducted in the absence of any commercial or financial relationships that could be construed as a potential conflict of interest.

References

1. Xiong, J.; Lu, X.; Li, W.; Yang, S.; Zhang, R.; Li, X.; Han, J.; Li, D.; Yu, Z. One-Pot Tandem Transformation of Inulin as Fructose-Rich Platform Towards 5-Hydroxymethylfurfural: Feedstock Advantages, Acid-Site Regulation and Solvent Effects. *ChemSusChem* **2023**, *16*, e202201936. [CrossRef] [PubMed]
2. Wang, Y.; Zhang, C.; Cai, C.; Huang, C.; Shen, X.; Lou, H.; Hu, C.; Pan, X.; Wang, F.; Xie, J. Advances in Humins Formation Mechanism, Inhibition Strategies, and Value-Added Applications. *Chin. J. Catal.* **2025**, *71*, 25–53. [CrossRef]
3. Zuo, M.; Lin, L.; Zeng, X. The Synthesis of Potential Biofuel 5-Ethoxymethylfurfural: A Review. *Fuel* **2023**, *343*, 127863. [CrossRef]
4. Ma, C.; Hu, J.; Wang, H.; Yu, Y.; Tan, C. Advances and Challenges in Biomass Thermochemical Conversion: From Resource Utilization to Process Optimization. *Renew. Sustain. Energy Rev.* **2026**, *226*, 116385. [CrossRef]
5. He, H.-L.; Deng, L.; Luo, Y.; Liu, Q.; Zhu, X.; Wang, L. Separation and Purification of 5-Hydroxymethylfurfural by Metal–Organic Frameworks. *J. Mater. Chem. A* **2025**, *13*, 36307–36317. [CrossRef]
6. Chen, C.; Lv, M.; Hu, H.; Huai, L.; Zhu, B.; Fan, S.; Wang, Q.; Zhang, J. 5-Hydroxymethylfurfural and Its Downstream Chemicals: A Review of Catalytic Routes. *Adv. Mater.* **2024**, *36*, 2311464. [CrossRef]
7. Cadu, A.; Sekine, K.; Mormul, J.; Ohlmann, D.M.; Schaub, T.; Hashmi, A.S.K. Homogeneous Catalysed Hydrogenation of HMF. *Green Chem.* **2018**, *20*, 3386–3393. [CrossRef]
8. Neukum, D.; Lakshmi Nilayam, A.R.; Ludwig, M.E.; Vadarlis, A.A.; Grunwaldt, J.-D.; Saraçi, E. Continuous Flow Oxidation of HMF Using a Supported AuPd-Alloy. *Catal. Sci. Technol.* **2024**, *14*, 2130–2138. [CrossRef]
9. Allen, M.C.; Hoffman, A.J.; Liu, T.; Webber, M.S.; Hibbitts, D.; Schwartz, T.J. Highly Selective Cross-Etherification of 5-Hydroxymethylfurfural with Ethanol. *ACS Catal.* **2020**, *10*, 6771–6785. [CrossRef]
10. Annatelli, M.; Trapasso, G.; Torre, D.D.; Pietrobon, L.; Redolfi-Bristol, D.; Aricò, F. A Green Synthesis of 5,5′-[Oxybis(Methylene)]Bis-2-Furfural: From By-Product to Attractive Bio-Based Platform Chemical. *Adv. Sustain. Syst.* **2022**, *6*, 2200297. [CrossRef]
11. Lin, Y.; Gong, X.; Chen, Y.; Wu, X.; Lu, D.; Yu, J.; Weng, R.; Zhang, Y.; Wang, F.; Xu, G. Promotion and Stabilization of High-Valence CoO_2 for the Efficient Electrooxidation of 5-Hydroxymethylfurfural (HMF) toward 2,5-Furandicarboxylic Acid (FDCA). *ACS Sustain. Chem. Eng.* **2025**, *13*, 21706–21714. [CrossRef]
12. Carro, J.; Fernández-Fueyo, E.; Fernández-Alonso, C.; Cañada, J.; Ullrich, R.; Hofrichter, M.; Alcalde, M.; Ferreira, P.; Martínez, A.T. Self-Sustained Enzymatic Cascade for the Production of 2,5-Furandicarboxylic Acid from 5-Methoxymethylfurfural. *Biotechnol. Biofuels* **2018**, *11*, 86. [CrossRef] [PubMed]
13. Giorgianni, G.; Van Putten, R.-J.; Van Der Waal, J.C.; Perathoner, S.; Centi, G.; Abate, S. The Conversion of 5-Chloromethylfurfural Into 5-Methoxymethylfurfural via Nucleophilic Substitution: Kinetic Modelling. *Chem. Eng. Trans.* **2024**, *109*, 265–270. [CrossRef]
14. Wei, J.; Wang, T.; Cao, X.; Liu, H.; Tang, X.; Sun, Y.; Zeng, X.; Lei, T.; Liu, S.; Lin, L. A Flexible Cu-Based Catalyst System for the Transformation of Fructose to Furanyl Ethers as Potential Bio-Fuels. *Appl. Catal. B Environ.* **2019**, *258*, 117793. [CrossRef]
15. Díaz-Maizkurrena, P.; Requies, J.M.; Iriondo, A.; Arias, P.L.; Mariscal, R. 5-Methoxymethyl Furfural Production by Acid Heterogeneous Catalytic Etherification of 5-Hydroxymethyl Furfural. *Catal. Today* **2024**, *426*, 114374. [CrossRef]
16. Bicker, M.; Kaiser, D.; Ott, L.; Vogel, H. Dehydration of D-Fructose to Hydroxymethylfurfural in Sub- and Supercritical Fluids. *J. Supercrit. Fluids* **2005**, *36*, 118–126. [CrossRef]
17. Kraus, G.A.; Guney, T. A Direct Synthesis of 5-Alkoxymethylfurfural Ethers from Fructose via Sulfonic Acid-Functionalized Ionic Liquids. *Green Chem.* **2012**, *14*, 1593–1596. [CrossRef]
18. Zhang, L.; Zhu, Y.; Tian, L.; He, Y.; Wang, H.; Deng, F. One-Pot Alcoholysis of Carbohydrates to Biofuel 5-Ethoxymethylfufural and 5-Methoxymethylfufural via a Sulfonic Porous Polymer. *Fuel Process. Technol.* **2019**, *193*, 39–47. [CrossRef]
19. Zuo, M.; Zheng, X.; Che, W.; Wang, K.; Chen, Y.; Zeng, X. Insight into 5-Hydroxymethylfurfural Synthesis and Separation from the Aqueous Solvent with Ion Exchange Resin Catalysts, Mechanisms, and Theoretical Calculations. *Sep. Purif. Technol.* **2025**, *362*, 131904. [CrossRef]
20. Sonsiam, C.; Kaewchada, A.; Pumrod, S.; Jaree, A. Synthesis of 5-Hydroxymethylfurfural (5-HMF) from Fructose over Cation Exchange Resin in a Continuous Flow Reactor. *Chem. Eng. Process.-Process Intensif.* **2019**, *138*, 65–72. [CrossRef]
21. Zhu, H.; Cao, Q.; Li, C.; Mu, X. Acidic Resin-Catalysed Conversion of Fructose into Furan Derivatives in Low Boiling Point Solvents. *Carbohydr. Res.* **2011**, *346*, 2016–2018. [CrossRef]

22. Yang, H.; Zhou, F.; Chen, H.; Li, J.; Ma, H.; Chen, K.; Lu, X.; Ouyang, P.; Fu, J. Highly Efficient Production of 5-Methoxymethylfurfural from Fructose in Dimethyl Sulfoxide/Amberlyst-15 Catalytic System. *Ind. Eng. Chem. Res.* **2020**, *59*, 4905–4911. [CrossRef]
23. Li, B.; Chen, Y.; Guan, W.; Wei, Y.; Zhang, Y.; Yan, Y. Hierarchical Porous Nitrogen-Doped Carbon Catalyst by the Pickering HIPE Technique: Synthesis and Application in HMF Production. *Energy Fuels* **2021**, *35*, 4191–4202. [CrossRef]
24. Kobkeatthawin, T.; Thiensuwan, N.; Chotirattanachote, A.; Chaowamalee, S.; Ngamcharussrivichai, C. Selectivity Control in Catalytic Glucose Dehydration Using Iron- and Tungsten-Modified ZSM-5 Catalysts. *Mater. Today Sustain.* **2024**, *28*, 101005. [CrossRef]
25. Deguchi, Y.; Kono, M.; Koizumi, Y.; Watanabe, Y.; Fujita, M.; Izato, Y.; Miyake, A. Study on Autocatalytic Decomposition of Dimethyl Sulfoxide (DMSO) II: Analysis of Intermediate Substances Obtained in the Induction Period and Investigations Regarding Formic Acid. *Org. Process Res. Dev.* **2021**, *25*, 2658–2668. [CrossRef]
26. Tong, X.; Li, Y. Efficient and Selective Dehydration of Fructose to 5-Hydroxymethylfurfural Catalyzed by Brønsted-Acidic Ionic Liquids. *ChemSusChem* **2010**, *3*, 350–355. [CrossRef] [PubMed]
27. Chen, H.; Fu, L.; Hao, J.; Chen, X.; Chen, H.; Bian, K.; Ashagrie, T.A.; Guo, H.; Zhang, H.; Xiong, L.; et al. Hierarchically Porous Resin-Supported Solid Acid Catalysts: Optimal Sulfonation Strategy and Efficient Biodiesel Production from Oleic Acid via Tailored Esterification. *Energy Fuels* **2025**, *39*, 16267–16281. [CrossRef]
28. Largier, T.; Huang, F.; Kahn, W.; Cornelius, C.J. Poly(Phenylene) Synthesized Using Diels-Alder Chemistry and Its Sulfonation: Sulfonate Group Complexation with Metal Counter-Ions, Physical Properties, and Gas Transport. *J. Membr. Sci.* **2019**, *572*, 320–331. [CrossRef]
29. Li, X.; Zhu, Y.; Xia, D.; Wang, Z.; Zhang, G. Amino-Anchored Sulfonic Acid-Functionalized Heteropolyacid Ionic Liquid: A Highly Selective and Recyclable Catalyst for the Baeyer-Villiger Oxidation of Cyclohexanone. *J. Ind. Eng. Chem.* **2023**, *127*, 426–437. [CrossRef]
30. Xiang, Y.; Wen, S.; Tian, Y.; Zhao, K.; Guo, D.; Cheng, F.; Xu, Q.; Liu, X.; Yin, D. Efficient Synthesis of 5-Ethoxymethylfurfural from Biomass-Derived 5-Hydroxymethylfurfural over Sulfonated Organic Polymer Catalyst. *RSC Adv.* **2021**, *11*, 3585–3595. [CrossRef]
31. Montes-Campos, H.; Méndez-Morales, T.; Varela, L.M.; Ortuño, M.A. Role of Anions in 5-Hydroxymethylfurfural Solvation in Ionic Liquids from Molecular Dynamics Simulations. *Adv. Theory Simul.* **2022**, *5*, 2200522. [CrossRef]
32. Wu, J.; Yang, R.; Zhao, S.; Chen, W.; Chen, Z.; Chang, C.; Wu, H. Efficient Conversion of Fructose to Produce High-Purity 5-Hydroxymethylfurfural under Low Temperature. *Biomass Convers. Biorefin.* **2024**, *14*, 20143–20151. [CrossRef]
33. Li, L.; Hu, Y.; Li, H.; Hu, P.; Xue, Z.; Wu, D.; Hu, C.; Zhu, L. Probing the Formation of Soluble Humins in Catalytic Dehydration of Fructose to 5-Hydroxymethylfurfural over HZSM-5 Catalyst. *Fuel* **2023**, *344*, 128133. [CrossRef]
34. Dong, W.; Blasius, J.; Fan, Z.; Wylie, L. Vibrational Spectra Simulations in Amino Acid-Based Imidazolium Ionic Liquids. *J. Phys. Chem. B* **2024**, *128*, 6560–6566. [CrossRef] [PubMed]
35. Cai, B.; Feng, J.; Guo, D.; Wang, S.; Ma, T.; Eberhardt, T.L.; Pan, H. Highly Efficient Isomerization of Glucose to Fructose over a Novel Aluminum Doped Graphitic Carbon Nitride Bifunctional Catalyst. *J. Clean. Prod.* **2022**, *346*, 131144. [CrossRef]
36. Cai, J.; Xu, C.; Shi, W.; Wu, S. Selective HMF Synthesis from Glucose via Microwave-Assisted Metal Chloride Catalysis. *Biomass Bioenergy* **2024**, *181*, 107060. [CrossRef]
37. Kirdant, S.P.; Ghadge, S.S.; Jadhav, V.H. Graphitic-C_3N_4/γ-Al_2O_3 Composite Catalyst for Synthesis of 5-(Hydroxymethyl)Furfural from D-Glucose. *Energy Fuels* **2025**, *39*, 8529–8539. [CrossRef]
38. Sun, W.; Xu, J.; Li, L.; Liu, Z.; Xiao, Z.; An, Q.; Huang, J. Production of 5,5′(Oxy-Bis(Methylene)) Bis-2-Furfural from 5-Hydroxymethylfurfural through the Hydrogen-Bonding Catalysis of Ionic Liquids. *Mol. Catal.* **2025**, *573*, 114842. [CrossRef]

Disclaimer/Publisher's Note: The statements, opinions and data contained in all publications are solely those of the individual author(s) and contributor(s) and not of MDPI and/or the editor(s). MDPI and/or the editor(s) disclaim responsibility for any injury to people or property resulting from any ideas, methods, instructions or products referred to in the content.